(Received 8 June 2024, Accepted 17 July 2024, Scheduled 1 August 2024)

Iron Loss in Electrical Machine — Influencing Factors, Model, and Measurement

Jiawei Yi[1], Qinyuan Dong[1], Jianhua Sun[2], Lixia Sun[2,3], Xiang Li[1], Hui Hwang Goh[1], Haisen Zhao[4], Thomas Wu[1], and Dongdong Zhang[1,*]

[1] *The School of electrical engineering, Guangxi University, Nanning 530004, China*
[2] *College of Chemistry and Chemical Engineering, Guangxi University, Nanning 530004, China*
[3] *Guangxi Key Laboratory of Petrochemical Resources Processing and Process Strengthening Technology Guangxi University, Nanning 530004, China*
[4] *The State Key Laboratory of Alternate Electrical Supply System with Renewable Energy Sources North China Electric Power University, 102206, China*

ABSTRACT: Improving the efficiency of electrical machine is an important way to reduce carbon emissions. Accurate calculation and measurement of iron loss is an important part of improving efficiency of electrical machine. Therefore, how to accurately calculate and optimize the device structure to reduce iron loss has become a research focus. In this study, the influence of power supply, motor structure, ferromagnetic material, manufacturing processes, and multiphysics on the motor iron loss is discussed and summarized. Then, the classification and summary of the existing iron loss models are discussed, and shortcomings and the future research direction are suggested. In addition, several induction motor efficiency measurement standards are described, and the defects and improvement direction of efficiency measurement of converter-fed motor are discussed. The contents discussed and summarized in this study can be helpful to engineers engaged in high efficiency motor design and motor driving algorithm development.

1. INTRODUCTION

Achieving the Paris climate goals requires significant reductions in carbon dioxide (CO2) emissions [1], and reducing electricity consumption is the primary goal of decarbonization. As the main electromechanical conversion device, motors provide power for a variety of equipment and are widely used in industries, commerce, transportation, public services, and household appliances [2, 3]. A number of studies have shown that the improvement of motor efficiency has great energy saving potential [4, 5]. One way to improve motor efficiency is to reduce losses by optimizing motor structure during motor design stage [6, 7], and the other way is to optimize system operation by energy-saving operation strategy during motor operation [8, 9], in which motor loss model is involved in both.

The losses of the motor mainly include copper loss, iron loss, and mechanical loss, among which the analysis method of iron loss is the most complex, especially after the wide application of frequency conversion modulation technology [10]. There are a large number of iron loss models, each of which has advantages and disadvantages. For electrical machines engineers in different subdivisions, it is difficult to choose the appropriate iron loss model. Therefore, an overview of motor iron loss is needed. A large number of iron loss models were reviewed in [11, 12], and the advantages and disadvantages of each model as well as the scope of application were discussed in detail. However, in recent years, new progress has been made in iron loss model. The variable coefficient iron loss model, Preisach model, and Jiles/Atherton (J-A) model are not discussed and summarized in detail in literature [11, 12]. Ref. [13] reviews common magnetic core materials used in high-power high-frequency transformers, iron loss modeling methods based on Steinmetz equation (SE), and advanced core loss measurement techniques. Ref. [14] reviews and discusses the material characteristics, iron loss model, and simulation software used in ferromagnetic components of power electronic devices. However, the motor is a rotating equipment, compared with the transformer and other static equipment, and the iron loss caused by the rotating magnetic field in the motor is the calculation difficulty. For a motor, especially an electric vehicle motor, its speed range is wide, and it is difficult to establish the iron loss model suitable for a wide frequency range. Ref. [15] has extensively investigated the measurement and modeling of rotating core loss in motor, discussed several modeling methods of rotating core loss, and summarized four main methods of measuring rotating core loss.

However, the above review papers are not comprehensive. In the past decade, segmental variable coefficient iron loss model, high-speed motor iron loss model considering multiple physical fields [16], analytical iron loss model for optimal efficiency of motor system [17, 18], and newly developed hysteresis model have been widely proposed and applied to the design stage of motor and system operation stage. These new iron models need to be summarized to facilitate electrical engineers to better choose the corresponding iron loss models.

* Corresponding author: Dongdong Zhang (dongdongzhang@gxu.edu.cn).

This study focuses on the analysis, calculation, and measurement of motor core loss. First of all, this paper discusses the influence of Pulse Width Modulation (PWM) power supply, ferromagnetic material composition, motor structure, processing mode, multi-physical field, and other factors on iron loss. Then, we focus on the relatively new iron loss models in recent years compared with [14] and [15], discuss the current research deficiencies, and suggest future research directions. Finally, a critical voice is proposed for the existing converter-fed motor loss separation specification.

2. INFLUENCE OF DIFFERENT FACTORS ON IRON LOSS

The premise of accurate calculation of iron loss is to understand the factors affecting the iron loss of the motor in detail. The difficulty of iron loss analysis of converter-fed motor lies in the complex temporal and spatial harmonics in the motor magnetic field, which causes an additional harmonic loss in the motor core. In addition, the manufacturing processes will lead to the deterioration of ferromagnetic material performance, which will also have a great impact on the motor iron loss [19].

2.1. The Influence of Power Supply Mode on Iron Loss

Firstly, the influence of power supply mode on iron loss of motor is discussed. The power supply mode of the motor determines the magnetic field inside the motor core. Many studies have carried out relevant studies on the analysis and calculation of iron loss under PWM power supply [20]. Ref. [21] studied the influence of modulation index of PWM waveform and switching frequency on iron loss by using measured data. The results show that the iron loss decreases with the increase of modulation index, and the switching frequency has little effect on the iron loss. Further studies in [22] show that the increase of modulation index will lead to the decrease of the Minor hysteresis loop size, thus reducing the iron loss. In addition, it is found that the influence of power electronic topology on iron loss is quite large, that is, the iron loss under bipolar PWM waveform is much higher than that under unipolar PWM waveform. This is because the bipolar PWM waveform has more harmonic content than unipolar PWM waveform, which leads to the size of the minor loop in the hysteresis loop. Ref. [23] shows that the iron loss decreases slightly with the increase of switching frequency. Moreover, at very small values of the modulation index (less than 0.3), iron loss increases sharply.

2.2. The Influence of Motor Structure on Iron Loss

The influence of motor structure on iron loss of motor is mainly due to the space harmonic magnetic field. Motor slotting will lead to space harmonics in the motor core [24]. As known to all, the more the slots are, the lower the harmonic content is [25, 26]. Fractional pitch windings can eliminate some high harmonics [27], while distributed windings can reduce the magnetic density amplitude of harmonics [28]. In recent years, fractional slot concentrated winding (FSCW) structure has attracted wide attention in permanent magnet synchronous motor (PMSM) due to its high efficiency, short end-windings, and high slot fill factor [28]. Ref. [28] compares the FSCW motor performance with different winding layers and find that FSCW motor has a large rotor eddy current iron loss, and increasing the winding layer can reduce the rotor eddy current iron loss. New multiphase star-delta hybrid connection (SDHC) winding structure [29] and spatially shifted star triangle windings [30] suitable for FSCW have also been studied to reduce some low-order spatial harmonics in some air-gap flux density. In addition, flux barrier on the stator yoke [31], optimization method [32], and reasonable arrangement of magnetic slot wedges [33] can be adopted to weaken harmonics of air-gap flux density, thus reducing iron loss due to space harmonics from stator.

2.3. Influence of Material Properties on Iron Loss

The static and dynamic properties of ferromagnetic materials are determined by the structure and movement of the magnetic domains [34], which are characterized by the different magnetization curves and hysteresis loops of ferromagnetic materials. People are used to use coercivity, saturation magnetization, permeability, and resistivity to characterize the basic properties of ferromagnetic materials. All kinds of ferromagnetic materials with excellent properties in practice are obtained by external factors (cold working, heat treatment, grinding, orientation, etc.) affecting the magnetic domain structure under the condition of appropriate ferromagnetic material composition [35]. Different processing levels will lead to the great difference in the properties of ferromagnetic materials. The first is the grain size of the material. The larger the grain size is, the smaller the hysteresis loss is, but the eddy current loss is increased, and the coercivity is decreased [35]. Secondly, different processing levels will also lead to different contents of impurities in steel sheets [36]. The increase of impurity content will increase coercivity, reduce saturation magnetic induction intensity, and increase hysteresis loss [36]. However, different processes will lead to different mechanical properties of the steel sheet. It is difficult for the brittle steel sheet to be processed into a very thin silicon steel sheet [37]. However, a very thin steel sheet can greatly reduce eddy current loss [38]. Finally, during manufacturing, manufacturing processes introduce local strain as well as compressive and tensile stress, which will increase the coercivity and hysteresis loss [39].

The most widely used magnetic material for motors is alloy laminates, in which the main element is iron, and silicon (Si), aluminum (Al), nickel (Ni), cobalt (Co), and manganese (Mn) are often added to adjust the magnetic and mechanical properties [38]. The influence of different metal elements on the properties of ferromagnetic materials is discussed in detail in [38]. To sum up, the influence of ferromagnetic material parameters on its performance can be summarized as shown in Fig. 1.

2.4. Influence of Manufacturing Processes on Iron Loss

Commercial silicon steel sheets must undergo different processing procedures before they can be used in motors, as shown in Fig. 2, including cutting, welding, interlocking or gluing, which will deteriorate the magnetic properties of the steel sheets [39]. Ref. [40] comprehensively introduces the law of

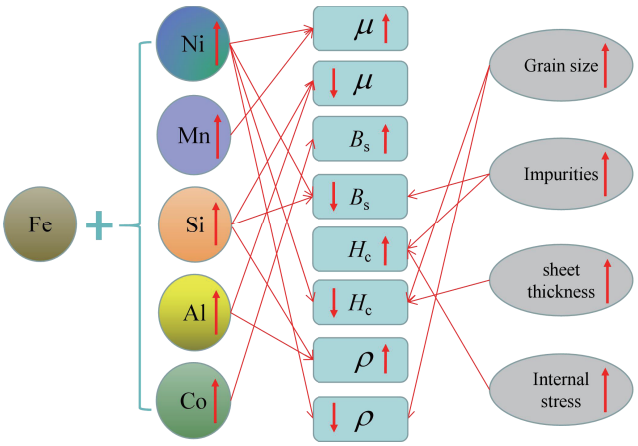

FIGURE 1. Influence of ferromagnetic material parameters on its properties. μ is the permeability; ρ is resistivity; B_s is saturation magnetization; H_c is coercive field strength.

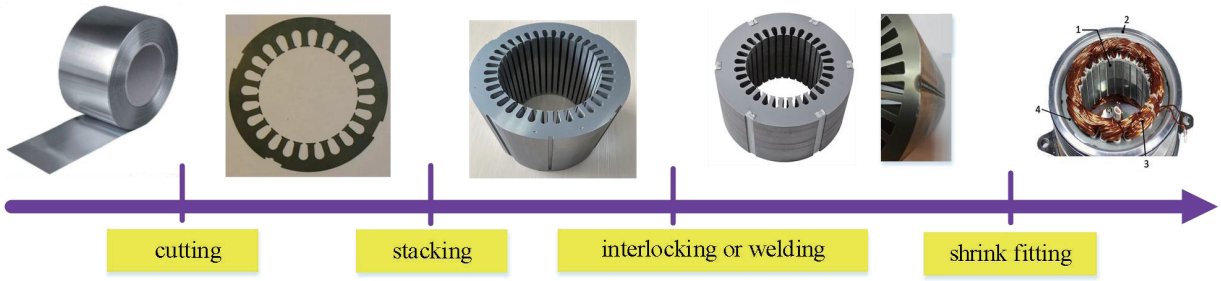

FIGURE 2. Motor stator manufacturing process.

the influence of cutting technology on the macro and micro characteristics of non-oriented silicon steel. The effects of cutting speed, tool wear state, laser type, and wire or spark of EDM on material properties are also discussed. Ref. [41] studies and reviews the influence of several main machining methods on the performance of motor core, and finds that Punching will produce mechanical stress on the steel sheets and affect its electromagnetic properties. Shrink will cause the frame to generate compressive stress on the stator, reduce the permeability of electrical steel, and increase the iron loss density. Welding will short-circuit the laminate surface of stator and increase eddy current loss. In addition, heat generated in the welding process will also generate thermal stress, resulting in a decrease in permeability and an increase in iron loss density. Ref. [42] find that blunt tools will increase static hysteresis loss. In addition, tool wear can cause slot edge burrs [42]. The more serious the tool wear is, the higher the burr height is, the more serious the short circuit is between the upper and lower layers of the silicon steel sheet, and the greater the eddy current loss is [42]. Ref. [43] studies in detail the effects of CO2 laser cutting, solid-state laser cutting (FKL) laser cutting, and mechanical cutting on magnetization characteristics and specific loss of electrical steel plates. It is found that the compressive stress of laser cutting is larger than that of mechanical cutting, which leads to larger static hysteresis loss and increases the resistance of silicon steel at the same time, so the eddy current will be reduced. Ref. [44] shows that laser cutting not only affects the loss of the magnetic core, but also affects the magnetization curve of the magnetic core at different frequencies. Ref. [45] shows that core loss increases more with the increase of laser cutting frequency, and the steel with high thermal conductivity will produce higher residual stress during laser cutting. There is now a form of gluing for ultra-thin silicon steel, which is used to laminated silicon steel sheets. Adhesive is beneficial to the performance of thin silicon steel, reduces the occurrence of eddy current, reduces the ability loss caused by welding, and plane bond mechanical strength is higher. Ref. [46] presents the methods used to represent the properties of the cut sheet for the finite element model (FEM) simulation, providing an alternative way to explore the effect of cutting process on magnetic material properties. Cutting deteriorates the magnetic properties of materials at the cutting edge. Ref. [47] analyzes and summarizes the deterioration depths presented in the literature. It not only provides an overview of the quantitative results, but also discusses them in the context of the respective measurement method.

2.5. Influence of Motor Multiphysics on Iron Loss

In the process of motor operation, the change of some physical parameters will also lead to some changes in the properties of ferromagnetic materials, which will lead to the error of the iron

TABLE 1. Influence of different factors on the lamination steels [38, 41].

Aspects	Factor	P_h	P_e	B_s	H_c
Power supply	Switching frequency (↗)	↘	↘		
	Modulation depth (↗)	↘			
Properties of lamination steels	Grain Size (↗)	↘	↗		↘
	Impurities (↗)	↗		↘	↗
	Sheet thickness (↗)	↘	↗		↘
	Internal stress (↗)	↗			↗
Alloy content	Silicon content (↗)		↘	↘	
	Aluminum content (↗)		↘	↘	
	Manganese content (↗)	↘	↗		↘
	Cobalt content (↗)			↗	
	Nickel content (↗)		↗		↘
Manufacturing Processes	Punching process	↗	↗	↘	
	Laser cutting	↗	↘		
	Pressing process	↗			
	Welding process	↗	↗		
	Shrink Fitting	↗			
Multiphysics	temperature	↘	↘		
	centrifugal stresses	↗			

P_h is Hysteresis losses; P_e is Eddy current losses (Including excess losses); B_s is Saturation magnetization; H_c is Coercive field strength.

loss model under static measurement. Ref. [48] shows that both hysteresis and eddy current losses vary linearly with temperature, and their loss coefficients fluctuate with flux density and frequency. In [49], the variation of iron loss of soft magnetic composite (SMC) with temperature is studied. It is found that the hysteresis loss and eddy current loss of SMC decrease with increasing temperature. Ref. [50] shows that the loss of thicker silicon steel is more affected by temperature. Refs. [16] and [51] show that eddy current loss coefficient is mainly related to temperature field, and hysteresis loss coefficient is strongly dependent on stress field. Ref. [52] shows that compressive stress has a greater effect on iron loss, while tensile stress has a lesser effect on iron loss. Ref. [53] shows that the centrifugal stress of the rotor will lead to a significant increase in the iron loss of the rotor at high rotational speed. Ref. [54] indicates that stacking stress reduces the permeability, resulting in a more specific loss, and that the reduction in permeability is nonlinearly related to the applied stress.

2.6. Summary of All Influencing Factors

To better summarize the influence of various factors on the performance of ferromagnetic materials, this study gives an overview through Table 1. Please note that Fig. 1 and Table 1 only represent the correlation (positive or negative correlation) of the influencing factors on the properties of ferromagnetic materials and do not represent specific values.

3. IRON LOSS MODELS OF ELECTRICAL MACHINES

Iron loss calculation is an important part of motor design to optimize motor structure and improve efficiency, and an important part of motor optimal efficiency control. Fig. 3 shows some commonly used iron loss calculation models over the years, from which we can clearly see the development and relationship of various iron loss models.

3.1. Steinmetz Equation

The first is the classical Steinmetz equation [55]. The early Steinmetz model was obtained under the assumption that the flux density waveform is pure sine, but the flux density in the actual motor is difficult to reach the pure sine waveform, so the model error is large. Therefore, many scholars have improved and perfected Steinmetz's model. Strengthened Steinmetz models include Modified Steinmetz Equation (MSE) [56], Generalized Steinmetz Equation (GSE) [57], Improved Generalized Steinmetz Equation (IGSE) [58], and Natural Steinmetz Extension (NSE) [59], and several enhanced versions of Steinmetz model have been introduced in detail in references [11, 60], which will not be repeated here.

3.2. Loss Separation Model

With the deepening of research, scholars began to study the mechanism of iron loss, and relevant scholars established the loss separation model according to physical mechanisms.

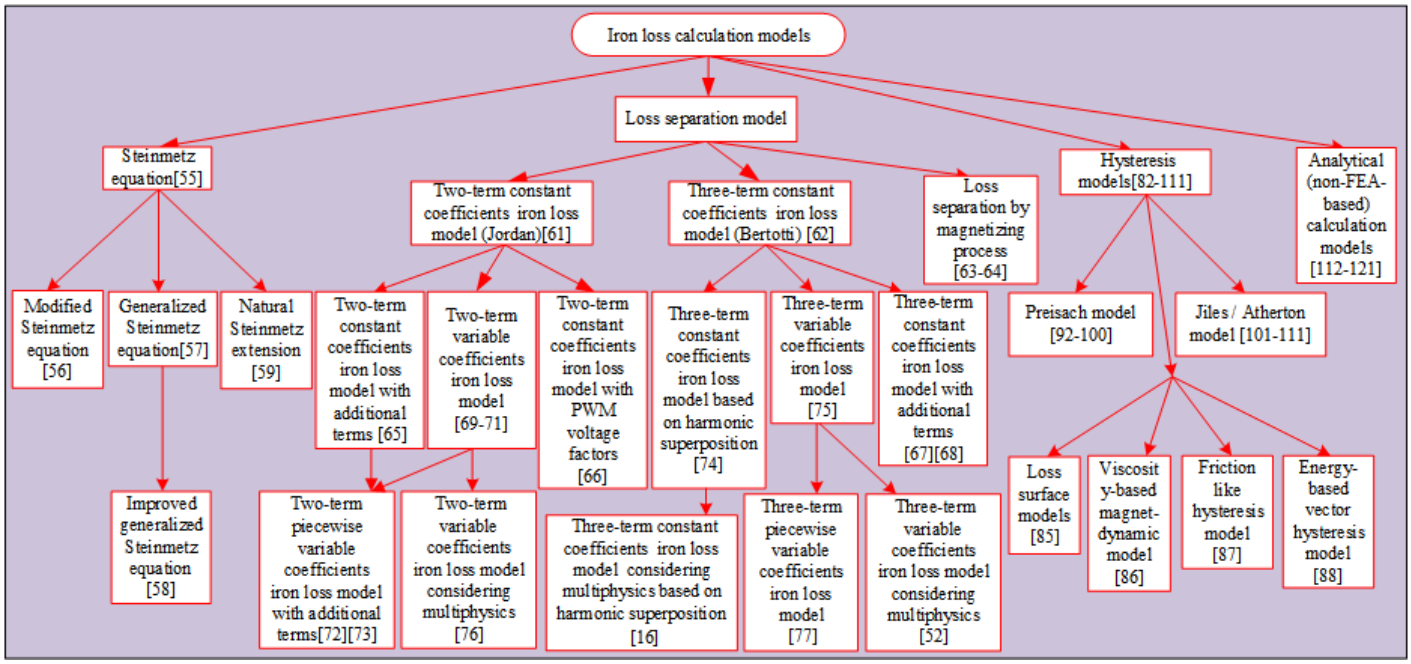

FIGURE 3. Iron loss models of electrical machines.

The classical loss separation models include two-term loss model [61] (Jordan's model), three-term loss model [62] (Bertotti's model), and loss model after magnetization [63, 64].

Compared with the Jordan's model, Bertotti's model added an excess loss, which took into account the loss caused by the domain wall motion and the time effect in the domain process. Both the Jordan's model and Bertotti's model assume that the ferromagnetic material works in the linear region without considering the influence of harmonic magnetic field. The saturation of ferromagnetic materials will increase the difficulty of eddy current loss calculation. The harmonic magnetic field will deform the hysteresis loop, as shown in Fig. 4, that is, there are many irregular small hysteresis loops, which leads to the difficulty of hysteresis loss modeling [65]. Ref. [66] proposes a two-term constant coefficient iron loss model based on voltage harmonic coefficient to consider the distortion of magnetic density of the core under variable frequency power supply. Refs. [67, 68] make a detailed analysis of the minor hysteresis loop caused by harmonic magnetic field and add additional high-order magnetic density term to the classical iron loss model to consider its influence. However, the coefficient of those model is constant, when the magnetic density varies widely, it is difficult to find an appropriate coefficient to meet the model accuracy under all magnetic density conditions. Therefore, the constant coefficient iron loss model does not have universal applicability.

To make the iron loss model have a higher accuracy in a wider range of frequency and magnetic density, a variable coefficient iron loss model is proposed in [69, 70]. The difference is that in [69] it is obtained that the hysteresis loss coefficient changes with the change of frequency and magnetic flux density, while the eddy current loss coefficient and excess loss coefficient change only with frequency. On this basis, [70] concludes that when the frequency is higher than 400 Hz, it is difficult to separate abnormal losses from eddy current losses, and the accuracy of three-term variable coefficient iron loss model becomes worse in high frequency band. A two-term variable coefficient iron loss model is proposed, in which excess losses are considered together with eddy current losses instead of being ignored. However, the coefficients of the above variable coefficient iron loss model are obtained by polynomial fitting method of magnetic flux density peak and frequency, which has its inherent defects [71], that is, when the magnetic density peak

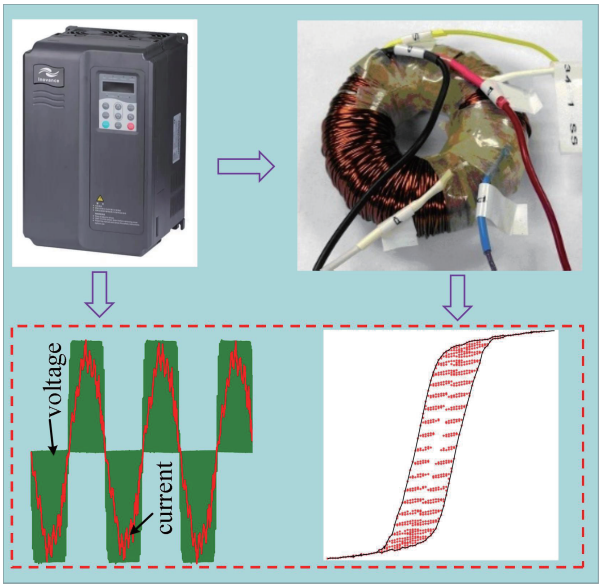

FIGURE 4. PWM harmonics lead to hysteresis minor loops in hysteresis curves.

value or frequency change is bigger, the ill-fitting will be more serious, and obvious errors will be produced.

In addition, the above variable coefficient iron loss model adopts the variable coefficient method to pursue the accuracy of the model from a mathematical point of view but does not put forward a clear compensation term [72], ignoring its physical significance. To further improve the accuracy of the model and clarify the influence of magnetic material saturation and harmonic magnetic field, the motor iron loss can be refined and analyzed [73]. Refs. [72, 73] propose a piecewise variable coefficient iron loss model, in which two additional flux density terms are introduced, and the nonlinear effect of materials and the effect of harmonic fields are considered. The hysteresis and eddy loss are compensated by different compensation coefficients in each magnetic density or frequency segment. Another significant advantage of this method is that the formula is directly applied to the finite element model, so the accuracy of iron loss is further improved while the physical significance of the model is not lost.

With the increase of motor speed, the fundamental frequency of motor increases, and the demagnetization effect at high frequency is a significant problem. Due to the high frequency demagnetization effect, the magnetic density is not evenly distributed on the axial plane, which is difficult to be solved by traditional modeling methods. High speed motor heat dissipation difficulty and high centrifugal stress will lead to the change of iron loss. Therefore, the calculation of iron loss of high speed motor has been studied in many researches. Based on Bertotti's iron loss model, [74] also adopted the orthogonal decomposition model to consider the influence of rotating magnetization, carried out coefficient fitting at different frequencies, and carried out the calculation and verification of iron loss of high-power high-speed motor. Ref. [75] deduces an analytical method for predicting the iron loss of the stator core of a slotless permanent magnet motor. It combines analytical solutions with variable-coefficient loss models or constant-coefficient loss models for efficient calculation through vectorization post-processing. Based on Bertotti's iron loss model, [16] established an iron loss model considered the interaction of multiple physical factors (high frequency, temperature and compressive stress). Based on the finite element method, [76] proposes a two-term variable coefficient iron loss model considering physical factors such as stress and temperature. The variable permeability is introduced into the skin effect coefficient to reflect the influence of flux density on eddy current loss, and the piecewise function was avoided. In [77], an improved three-term core loss model with piecewise-variable parameters based on finite element is proposed. Other iron loss models further consider the DC bias flux density [78] and use linear fitting and two-dimensional interpolation methods [79] to further improve the accuracy of the model.

Another separation calculation method of iron loss is called loss separation method after magnetization [80, 81], that is, the iron loss after magnetization is divided into linear magnetization, rotary magnetization, and the loss caused by high order harmonics. This iron loss model also takes into account the influence of rotating magnetization of the motor and harmonic magnetic field inside the motor, but its applicable frequency range will change with different models, which does not actually solve the problem that the iron loss model cannot be applied to a wider frequency range [80, 81].

3.3. Hysteresis Mathematical Model

Another method of calculating iron loss is the hysteresis model, which is based on measured material data and also includes various types. In these models, Jiles-Atherton (J-A) model [82] and Preisach model [83] are the most popular. Compared with other curve fitting models, these two methods can get accurate results and can be directly used in finite element simulation. Hysteresis mathematical model includes Dynamic Preisach Model [84], Loss Surface Model [85], Magneto dynamic Viscosity Based Model [86], Friction Like Hysteresis model [87], and Energy Based Hysteresis model [88]. For more details about these models, please refer to [14, 88]. In recent years, Preisach model and Jiles/Atherton model have been refocused on the hysteresis model. Ref. [89] compares the two models in terms of magnetic dynamics. Ref. [90] compares the comprehensive realization effects of the two models, summarizes the advantages and disadvantages of the two models, and provides a direction for subsequent research. Some scholars have also tried to synthesize the advantages of Preisach model and Jiles/Atherton model and established a new model integrating the advantages of the two models [91].

Firstly, the Preisach model is discussed. The Preisach model has high computational accuracy and can be applied to a wider range of materials, but it also tests the computing speed, storage and programming ability of the computer. In order to solve the defects of Preisach model applied in finite element, the key problems of Preisach model in finite element application are discussed in detail in [92]. For the H-based Preisach model, [93] simplifies the algorithm by eliminating search and interpolation schemes and improved the convergence, showing faster calculation time and better numerical convergence in finite element simulation. In [94], Preisach-Mayergoyz model is improved to improve its numerical performance in 3D finite element. In hysteresis analysis, Preisach model with variables is commonly used. However, this model may be affected by numerical instability or degenerate convergence when calculating magnetization as an input function of external magnetic field [91]. Ref. [95] proposes the method of replacing conventional M-H variables with M-B variables to improve the numerical stability in the iterative process. In [96], a generalized dynamic hysteresis model is proposed and applied to numerical analysis aiming at the Viscous Preisach model by applying fixed point iteration to finite element simulation. The application scope of the model is enlarged. At first, the Preisach model was proposed as a scalar model. However, the rotary motor has both alternating magnetic field and rotating magnetic field, and the combination of the two will produce vector hysteresis characteristics [97]. The vector Preisach model is proposed based on the scalar Preisach model [98]. Scalar Preisach model is the main building block of vector model, and vector model is the superposition of scalar model [99]. Ref. [100] proposes an improved vector Preisach hysteresis model considering the

TABLE 2. Summary of Preisach and Jiles-Atherton (J-A) models.

Preisach model		Jiles-Atherton (J-A) model	
[92]	Ansysed defects of Preisach model applied in finite element	[101, 102]	Solved the numerical convergence problem in finite element simulation
H-based Preisach model [93]	Improved the convergence	[103]	Introduces the numerical processing method of correlation tensor of vector J-A model used in finite Element method (FEM)
Preisach-mayergoyz model [94]	Improve its numerical performance in 3D finite element	[104, 105]	Identify the parameters of the Jiles-Atherton model
Preisach model with M-B variables [95]	Improve the numerical stability in the iterative process	[107, 108]	Predict the alternating and rotating iron loss in unoriented silicon steel sheet
Generalized dynamic hysteresis Model [96]	The application scope of the model is enlarged	[110]	Improve model accuracy under arbitrary frequency
Vector Preisach model [99, 100]	The effect of rotating magnetization can be considered	Dynamic hysteresis model [111]	Combined the instantaneous eddy current and residual loss model

anisotropy properties of SMC materials under vector magnetic excitation. By introducing two parameters, w and z, the vector Everett function is identified, and the hysteresis curve shapes under different flux densities are adjusted to further improve the accuracy of the model.

Compared with Preisach model, Jiles/Atherton (J-A) model relies on fewer parameters, is easy to implement numerically, and is fast in calculation, but is applicable to a narrower range of materials. Like Preisach model, J-A model also has numerical convergence problem in finite element simulation calculation. For this reason, Ref. [101] proposes a rule-based differential permeability value adjustment algorithm by using fixed point iteration method, which eliminates or reduces unnecessary disturbance to the calculated differential permeability value and ensures the convergence of the algorithm. In [102], the reasons for numerical non-convergence are analyzed, and the quasi-Newton method is introduced to accelerate the solution of nonlinear field equations, which not only ensures the stability of the algorithm but also improves the calculation speed. Ref. [103] introduces the numerical processing method of correlation tensor of vector J-A model used in finite Element method (FEM) based on 3D differential permeability formula. Ref. [104] combines false position method and iterative algorithm to identify the parameters of the classical model and the modified model. Ref. [105] proposes a constraint condition for convergence of J-A hysteresis model combined with finite element method and applies it to the classical determination method of parameter process of J-A hysteresis model. Ref. [106] proposes an electrical-magnetic-thermal-mechanical coupling J-A dynamic model with excitation current as input and displacement as output. According to the characteristics of the hysteresis loop, the unknown parameters are identified by differential evolution genetic algorithm. Ref. [107] proposes an improved vector J-A model, whose parameters are modified twice under alternating unsaturated rotation excitation and saturated rotation excitation, respectively, and the non-hysteretic magnetization function is improved, further improving the accuracy of the J-A model. Ref. [108] modifies the vector extension of J-A hysteresis model to predict the variation of alternating and rotating field strength in unoriented silicon steel sheet. In [109], an improved J-A model is proposed to improve the consistency between experimental and calculated results by introducing a scale factor into the hysteresis magnetization, especially at low Magnetic flux density. Ref. [110] proposes a simple method based on J-A model equation to predict iron loss under arbitrary frequency and compressive stress. To calculate the core loss accurately, [111] combines the traditional J-A hysteresis model with the instantaneous eddy current and residual loss model to establish a dynamic hysteresis model, which is applied to the finite element algorithm. The studies of Preisach and Jiles-Atherton (J-A) models are summarized in Table 2.

3.4. Analytical Calculation Method

The fast analytic iron loss calculation model is usually considered by the control algorithm, and then the optimization algorithm is used to optimize the overall loss control of the motor system, as shown in Fig. 5.

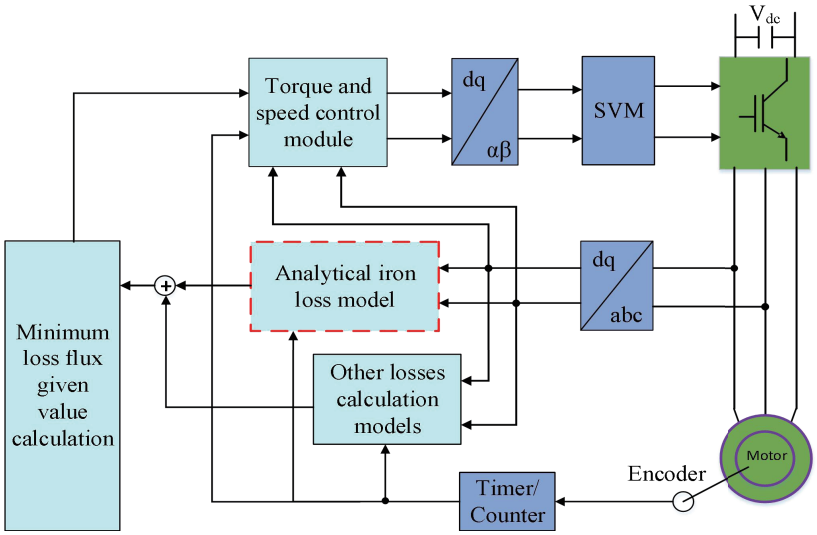

FIGURE 5. Schematic diagram of motor optimal efficiency control.

In order to establish the iron loss model suitable for the control algorithm, it is a common way to convert the magnetic density to voltage according to the motor geometry. In [112], a fast-analytical iron loss calculation model is proposed, which takes the output voltage of the inverter and motor speed as variables. In [113], in order to further reduce the calculation, two PWM voltage dependent coefficients are introduced to avoid the complexity of fitting the loss coefficient in Fourier superposition calculation. In [114], Cauer circuit model is applied to iron loss estimation of interior permanent magnet synchronous motor powered by PWM supply. This modeling method can obtain basically the same iron loss with lower computational cost. For the motor, the more advanced vector control mode is to decouple the three phases of the symmetrical rotation vector into the quadrature axis and the direct axis component. Ref. [115] establishes a new d-q axis model considering harmonic iron loss resistance for permanent magnet motors used in electric vehicles. Ref. [116] proposes a model for random dq0 frame analysis and core loss estimation under the condition of online feed and inverter power supply. Ref. [117] uses the function of Id, Iq current to describe the nonlinear iron loss coefficient. The early stages of motor design also require rapid analytical iron loss models to participate in the evaluation of motor efficiency. In [118], the influence of DC magnetic bias is considered, and the core loss under load and no-load conditions in post-processing is calculated by using Bertotti's model and magnetic flux change trajectory through analytical calculation of magnetic field. In order to build an accurate iron loss model suitable for wide speed range, [119] introduces the concept of fractional derivative into the simulation of classical eddy current losses in low and high frequency domains. In order to carry out the fine analysis of the motor in the motor design stage, the reluctance network model coupled with the analytical calculation model [120] and the subdomain model [121] are used to calculate and analyze the iron loss of each part of the motor.

3.5. Summary of All Models

The above iron loss models can be mainly divided into four categories, namely Steinmetz model, loss separation model, Hysteresis loss model, and analytical calculation model. The four types of iron loss models are summarized as follows:

a) Steinmetz model is only applicable to the calculation of motor iron loss under pure sinusoidal flux density at first. Although various improved Steinmetz models have been proposed since then, they are still not applicable to the calculation of iron losses with large harmonic magnetic fields, and the range of application of the model to ferromagnetic materials is limited. However, as the first proposed calculation model of iron loss, the historical significance of Steinmetz model is huge. Steinmetz model is simple, convenient, and easy to implement numerically, and can be easily implanted into finite element simulation. It can be used to estimate iron loss on some occasions where the calculation accuracy of iron loss is not high.

b) Jordan's model and Bertotti's model separate different iron loss components according to different physical mechanism, which enriches the physical significance of iron loss. Although the coefficients of variable coefficient iron loss model are changed, the coefficient fitting will have pathological problems in the case of a large frequency variation range, resulting in a decrease in accuracy. The piecewise variable coefficient iron loss model can solve the ill-conditioned problem. However, the calculation accuracy depends on the number of segments. When the number of piecewise is higher, the amount of calculation will be greatly increased. Loss separation model is also simple, easy to implement numerically, easy to integrate into finite element simulations, and its computational accuracy varies from model to model.

c) For hysteresis loss model, Preisach Model and Jiles/Atherton (J-A) model are mainly introduced.

TABLE 3. Comparison of different iron loss models.

Iron loss model	Non-sinusoidal supply	Rotation magnetization	Frequency range	Material prior knowledge	Accuracy
Steinmetz equation [55]	×	×	Narrow	Small	Low
Modified Steinmetz equation [56]	√	×	Narrow	Small	Low- medium
Generalized Steinmetz equation [57]	√	×		Small	Medium
Improved generalized Steinmetz equation [58]	√	×	Narrow	Small	Low-medium
Natural Steinmetz extension equation [59]	√	×	Narrow	Small	Medium
Two-term constant coefficients model (Jordan) [61]	×	×	Narrow	Small-medium	Low-medium
Two-term constant coefficients model with additional terms [65]	√	√	Narrow	Medium	Medium
Two-term variable coefficients model [69–71]	√	×	Wide	Medium	Good
Two-term constant coefficients model with PWM voltage factors [66]	√	×	Narrow	Medium	Good
Two-term piecewise variable coefficients model with additional terms [72, 73]	√	√	Wide	Medium	Good
Two-term variable coefficients model considering multiphysics [76]	√	√	Wide	High	Good
Three-term constant coefficients model (Bertotti) [62]	×	×	Narrow- Medium	Medium	Low- medium
Three-term constant coefficients model with additional terms [67, 68]	√	√	Medium	Medium	Medium
Three-term variable coefficients model [75]	√	√	Medium	Medium	Good
Three-term constant coefficients model considering multiphysics based on harmonic superposition [16]	√	√	Medium	Medium	Good
Three-term piecewise variable coefficients model [77]	√	√	Wide	High	Good

Three-term variable coefficients model considering multiphysics [52]	√	×	Medium	Medium	Good
Preisach model [92–100]	√	Model-dependent	Wide	High	Good
Jiles/Atherton model [101–111]	√	Model-dependent	Wide	High	Good
Dynamic hysteresis model [111]	√	×	Wide	High	Good
Loss surface model [85]	√	×	Wide	High	Good
Magneto-dynamic Viscosity Based model [91]	√	×	Wide	High	Good
Friction like hysteresis model [87]	√	√	Wide	High	Good
Energy based vector hysteresis model [88]	√	√	Wide	High	Good
Loss separation after magnetizing processes [80, 81]	√	√	Model-dependent	Model-dependent	Model-dependent
Analytical calculation models [112–121]	Model-dependent	×	Model-dependent	Small	Model-dependent

Hysteresis loss model requires more historical data and measurement data of materials. Its accuracy is generally high, and the frequency range is wide. The complex hysteresis loss model is more suitable for accurate determination of iron loss in the process of mechanical design and evaluation. Compared with Jiles/Atherton (J-A) model, Preisach model is applicable to a wider range of materials and has higher computational accuracy. However, it is relatively difficult to be numerically analyzed, requiring more computing memory and longer computation time.

d) Analytical calculation model is an iron loss model represented by analytical functions based on various physical relationships and motor structure. Due to the direct modeling, only the basic physical properties of ferromagnetic materials are required, without all kinds of historical data and measurement data. Its applicable occasions, applicable frequency range, and model accuracy are related to the physical factors considered in the modeling, so it depends on the model itself. However, because this model is simple in calculation and does not need material historical data, it has great advantages in the field of systematic energy-saving control of motor.

To distinguish various iron loss models more conveniently, we compared them from five aspects, and the comparison results are shown in Table 3.

3.6. Development and Recommendations

Despite the large number of iron loss models, the existing models still have some defects or ignore some factors. Therefore, this paper believes that relevant research still needs to be improved in the following aspects:

1) Many iron loss models are based on Jordan's model and Bertotti's model, and their model coefficients are obtained by fitting loss data measured under the Epstein framework. However, according to Section 2.4, the influence of manufacturing processes will lead to a significant increase of the iron loss, which leads to large errors. There are few studies on iron loss models considering the influence of processing factors. Therefore, How to simulate the influence of machining factors on the properties of ferromagnetic materials in finite element software and how to establish the iron loss model considering machining factors are the research difficulties and also the focus of future research.

2) As for the hysteresis model, according to Table 2, many researches are devoted to the numerical stability and convergence of the hysteresis model. However, the problem that it requires a large amount of material and historical data has not been well solved. Although some material data may be provided by the material manufacturer, additional measurements are required for more data, such as data under rotational magnetization and data after superimposed DC bias.

3) Converter-fed motor and frequency converter are coupled together, and the influence of modulation model and driving algorithm on iron loss is direct. Therefore, it is very necessary to establish an iron loss model which is strongly coupled with PWM mode (including considering PWM sampling law, dead time setting, etc.), which is the key to construct the analytic harmonic additional iron loss.

4) In addition, many iron models use the magnetic density of the motor to calculate the iron loss, while the control algorithm is more to control the flux, voltage, current, and other variables

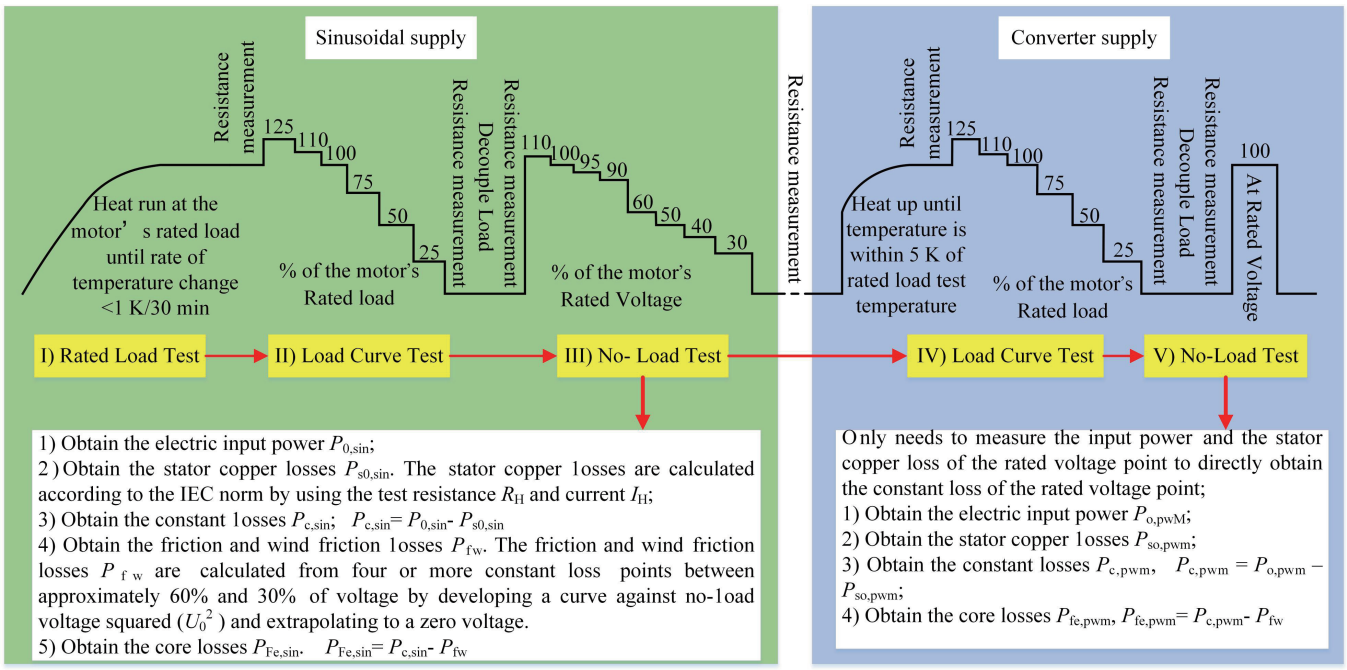

FIGURE 6. The detailed core loss measurement procedure [123].

of the motor. Simply converting magnetic density into voltage based on motor geometry is very rough, because the distribution of magnetic density inside the motor core is not uniform, which is also the reason for the high accuracy of finite element model calculation. However, for the control algorithm, the computational burden of finite element method is huge. Therefore, how to balance the accuracy of the model with the amount of computation and how to better implant the iron loss model into the control algorithm are the future research directions.

4. IRON LOSS SEGREGATION METHODOLOGY

The accurate measurement of iron loss is the basis of verifying the calculation model of iron loss and is also the key to determine the efficiency of the motor. Related standards such as IEEE 112, IEC 60404, and IEC 60034-2-1 have been in use for many years and have been consistently revised and improved [122]. However, although the efficiency measurement method of converter-fed induction motor has been introduced as a technical specification [123], there is still some time to go before the final standardization, and further discussion is still needed.

4.1. Differences between Steps in Loss Separation Standards

Although the standards for loss separation and efficiency measurement of induction motors may vary from region to region, they do not differ greatly. Almost all the loss separation standards under sinusoidal power supply can be basically divided into the following steps: stator winding resistance measurement at room temperature (Step I), temperature measurement at rated load (Step II), load curve test (Step III), and no load test (step IV). We listed several induction motor loss separation standards and made detailed comparison for each step, as shown in Table 4.

4.2. Test Specifications for Iron Loss Separation of Converter-Fed Motor

More recently, IEC/TS 60034-2-3 has been introduced as a technical specification of technical steps for loss separation of converter-fed motors. In IEC/TS 60034-2-3, the additional harmonic losses caused by a PWM supply are understood as the difference losses of a motor with a PWM supply and a sinusoidal power supply. According to the specification (IEC/TS 60034-2-3), we have sorted out the relevant parts of iron loss separation technology of converter-fed motor, as shown in Fig. 6 [123]. No-load test is the key step to separate iron loss. It is worth noting that IEC/TS 60034-2-3 also specifies the temperature correction factor for the stator copper loss (corrected to 25°C ambient temperature) [123]; also the influence of voltage drop of the stator winding on iron loss is taken into account [123].

4.3. Deficiency and Prospect

Many papers have provided valuable advice on IEC/TS 60034-2-3. Ref. [124] has read the IEC standard for efficiency measurement of induction motors and suggests that the efficiency measurement method provided by IEC cannot be used to predict the loss of variable speed drive (VSD) systems in end-user applications. Ref. [124] suggests that an automated process based on state machines should be used to manage the entire test because repeated steps of IEC/TS 60034-2-3 may cause of human error. Ref. [125] suggests that measurement equipment specified in IEC standards is complex and expensive, leading differ-

TABLE 4. Differences between steps in loss separation standards [122].

Standard	Cold resistance measurement	Rated load temperature test	Load curve test	No load test
IEC 60034-2-1: 2014 Method 2-1-1 B	Line-to-line winding resistance value at ambient temperature should be recorded	Input power, current, voltage, frequency, torque, speed, resistance values, winding temperature should be recorded until thermal equilibrium is achieved (the rate of winding temperature change 1 K or less per half hour)	• Apply the load to the machine at following six load points: approximately 125%, 115%, 100%, 75%, 50% and 25% of rated load • Measure resistance before the highest and after the lowest load reading	Under no-load condition, test the machine at the following eight voltage points: approximately 110%, 100%, 95%, 90%, 60%, 50%, 40% and 30% of rated voltage
IEEE-112 Method B	With the machine at ambient temperature, measure and recorded the winding resistance and ambient temperature	Almost same with IEC 60034-2-1: 2014 Method 2-1-1 B	• Apply the load to the machine at following four load points approximately equally spaced between not less than 25% and up to 100%, and two load points suitably chosen above 100% load but not exceeding 150% load • Perform the test as quickly as possible to minimize temperature changes in the machine during testing	Under no-load condition, test the machine at the voltage ranging from 125% of rated voltage down to point where further voltage reduction increases the current
CSA C390:2010	A motor shall be considered cold when the winding, stator core, or frame temperature is within $\pm 3^{\circ}$ of ambient temperature. Cold motor stator winding resistance and cold winding temperature should be recorded	Input power, current, voltage, frequency, torque, speed, resistance values, winding temperature should be recorded until thermal equilibrium is achieved (the rate of winding temperature change 1 K or less per half hour, or the rate of motor frame or core temperature change 1 K or less per half hour)	Almost same with IEEE-112 Method B	Under no-load condition, test the machine at three or more voltage points between 125% and 60% of rated voltage, with the middle point being as close as possible to 100% of rated voltage and three or more voltage points approximately equally spaced between 50% of rated voltage and 20% of rated voltage, or point where the line current reaches a minimum stable value

ent researchers to look for different methods to estimate efficiency rather than to carry out actual tests. Ref. [126] points out that IEC/TS loss separation using PWM power supplies may be more uncertain than indirect methods using sinusoidal power supplies, because no-load measurements (step V) of the converter power supply are tested only at rated points. Ref. [127] proposes an automated efficiency test procedure to mitigate the adverse effects of different technical skills and ability levels of testers on efficiency test results.

Based on IEC/TS 60034-2-3, this study further gives relevant opinions on the iron loss separation part:

1) First of all, it is necessary to increase the provisions related to iron loss separation methods under different load conditions. The IEC standard considers iron loss to be a constant loss that does not change with the load, which is a simplification of the procedure and not the truth. However, with the increase of the load, the distribution of magnetic flux changes significantly, resulting in an overall increase in the content of harmonic flux. Therefore, the variation law of magnetic core loss with load still needs to be studied and discussed [128].

2) An important reason that it is difficult to accurately calculate the iron loss of the motor is that it is difficult to obtain the correct parameters of the model, especially in the case of curve fitting. The loss coefficient is measured and fitted from the typical Epstein frame. However, the geometric structure of the motor is completely different from that of the Epstein frame. The complexity of the geometric structure will lead to more complex machining, and the increase of iron loss due to the complexity of machining is also one of the reasons for the imprecision of the model. Therefore, it is worth thinking and studying how to obtain more accurate model parameters by directly measuring the iron loss data of the motor.

3) According to the IEC 60404-6:2018 standard for Magnetic materials — Part 6: Measurement of magnetic soft metals and powder materials in the frequency range of 20 Hz to 100 kHz using ring samples, it is also worthwhile to explore how this standard can be extended to the test of iron loss in motor stator cores. This means that this test must be done before the motor is assembled, which simplifies the test procedure because there is no need to control the speed of the motor.

4) In addition, the determination method of additional harmonic iron loss of converter-fed motor should be more clearly defined. IEC/TS 60034-2-3 only provides the determination method of harmonic additional constant loss, does not clearly recognize its component, and the IEC/TS 60034-2-3 does not involve how to separate the additional harmonic iron loss from it.

5) Finally, the current relevant standards for motor efficiency are for induction motors. For other types of motors, the iron loss measurement has not been standardized [129, 130]. Especially for permanent magnet motors, because the rotor magnetic field is not adjustable, the conventional means of adjusting voltage to test the iron loss will lead to the increase of no-load rotor eddy current loss, which is coupled with the iron loss and difficult to separate. Therefore, how to accurately measure the iron loss of permanent magnet motor is also very challenging, which requires more researchers to invest more energy.

TABLE 5. Specification of the 5.5 kW Induction Motor with Laminated Steel DR510.

Number of poles	4
Number of phases	3
Number of stator slots	36
Number of rotor slots	32
Rated output power	5.5 kW
Rated phase current	11.64 A
Rated phase voltage	380 V
Rated efficiency	0.88
Power factor	0.85
Stator winding connection	Delta
Rated speed	1440 r/min
Stator outer diameter	210 mm
Stator bore diameter	136 mm
Active stack length	115 mm
Air-gap length	0.4 mm
Rotor length	117 mm

5. CASE STUDY

This study takes iron loss calculation of 5.5 kW frequency conversion feed induction motor as an example, and its parameters are shown in Table 5. The iron core of 5.5 kW induction motor is stacked with DR510. The iron loss modeling process is shown in Fig. 7. A 2D finite element simulation model is established by ANSYS/ Maxwell. We used a numerical analog computer (two Xeon E5-2690 V3 CPUS, 256GB OF RAM) for calculations. The bottom of the motor stator tooth and the top of the rotor tooth are selected as two typical positions, and the radial and tangential magnetic density waveforms of the two typical positions are extracted by using the finite element software, as shown in Fig. 8. Magnetic density extraction is carried out after the simulation model reaches a stable state. The transition process has 10 supply cycles, and the flux density data of the 11th cycle is used to calculate the motor iron loss. The

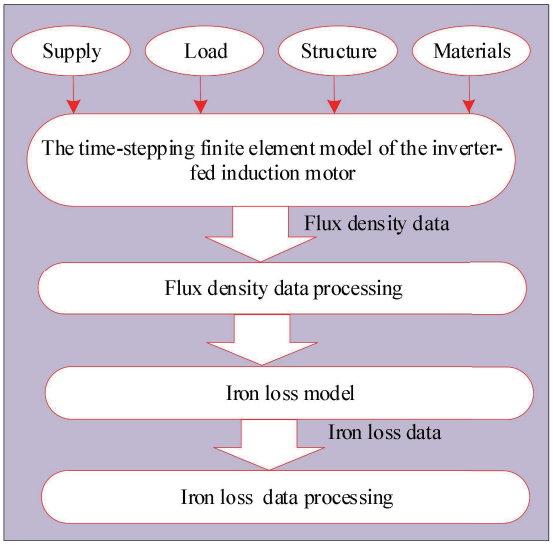

FIGURE 7. Iron loss modeling process.

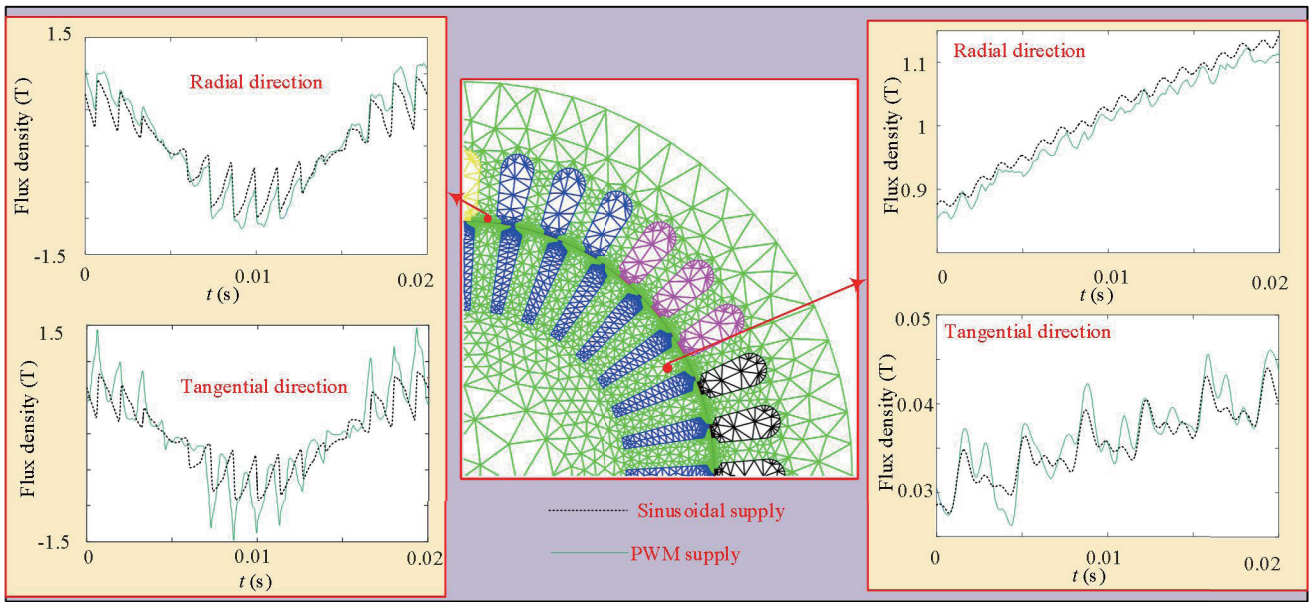

FIGURE 8. Magnetic density waveform of typical position of stator and rotor tooth in 5.5 kW converter-fed induction motor.

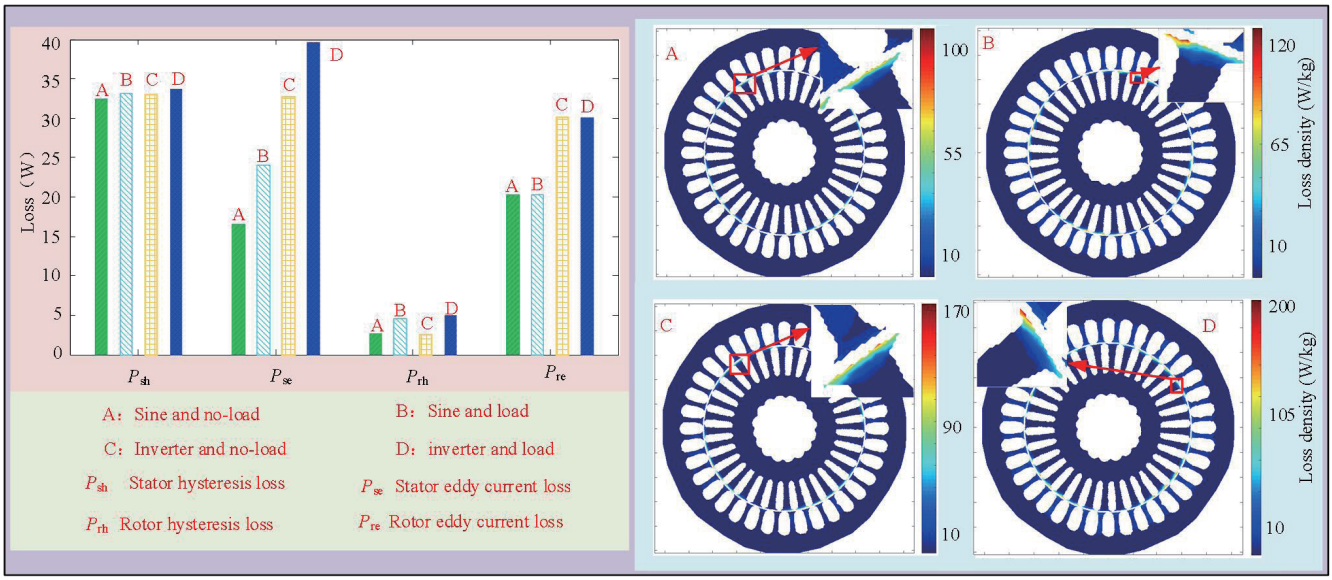

FIGURE 9. Iron loss components and loss density under different operating conditions of 5.5 kW induction motor.

iron loss of 5.5 kW motor was calculated by using the piecewise variable coefficient iron loss model in [72] and the classical two-term iron loss model respectively and compared with the measured value.

Firstly, by establishing the finite element model, the hysteresis loss and eddy current loss of 5.5 kW converter-fed induction motor are calculated by using the two-term piecewise variable coefficient iron loss (PVCIL) model [72] and the classical two-term iron loss (CIL) model. Fig. 9 shows the cloud diagram of iron loss density obtained by simulation and iron loss components obtained by calculation. Under the condition of inverter power supply, by changing the switching frequency of inverter, the iron loss components are calculated by two models respectively, and the iron loss of 5.5 kW induction motor is tested according to IEC/TS 60034-2-3. Fig. 10 shows the calculated results of iron loss at different switching frequencies and the comparison with the measured values. As shown in Fig. 9, the following conclusions can be drawn from the bar diagram of each iron loss component: at the stator side, eddy current loss is greatly affected by power supply mode and load, while hysteresis loss is less affected by it. For example, under sinusoidal power supply, the stator eddy current loss under load is 24 W,

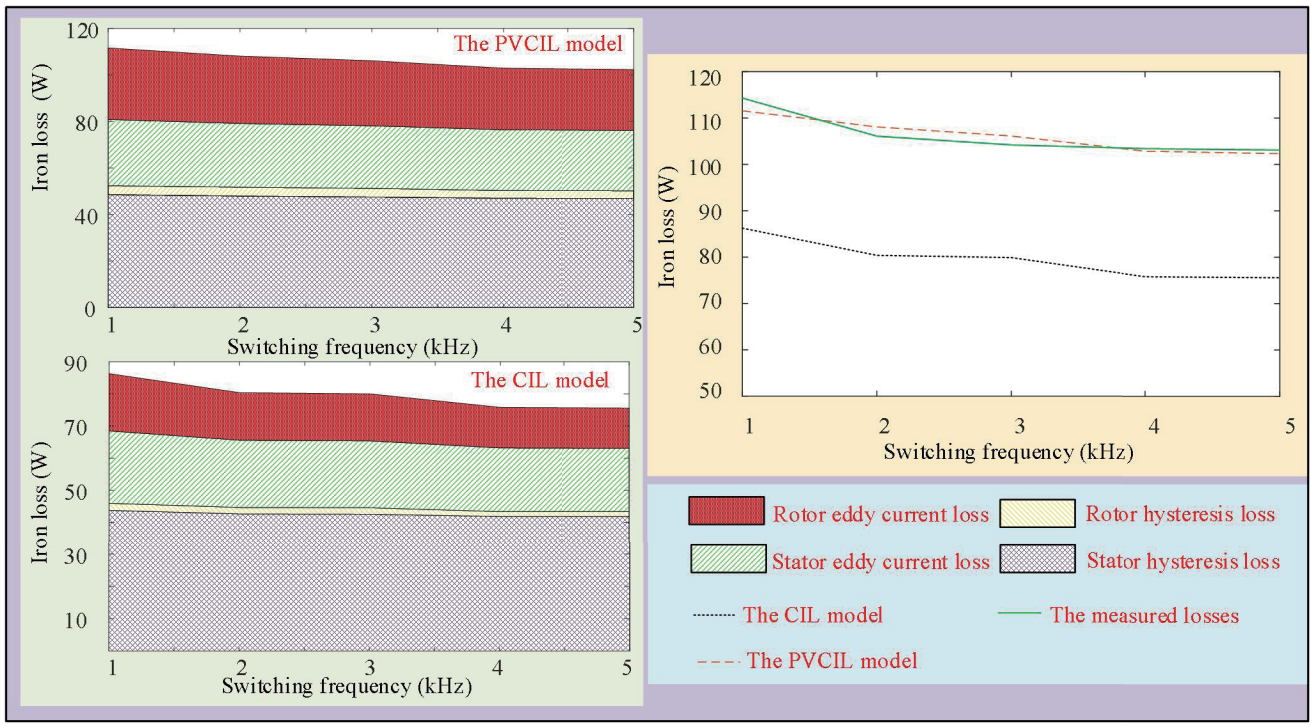

FIGURE 10. The change of iron loss of 5.5 kW converter-fed induction motor with switching frequency.

which is 41.2% higher than that under no load. In the case of load, the stator eddy current loss under inverter power supply is 39.5 W, which is 64.6% higher than that under sinusoidal power supply. The hysteresis loss of the stator is almost the same in the four cases. At the rotor side, hysteresis loss mainly depends on the load condition, while eddy current loss mainly depends on the PWM harmonics. According to the iron loss density cloud diagram of the motor, PWM power supply and load will lead to the increase of iron loss density. Load will lead to a slight increase in the maximum iron loss density of the motor, and the harmonic wave of the inverter has a greater influence on the local electromagnetic density. In the same condition, the iron loss density of rotor teeth, especially the tip near the motor air gap, is significantly higher than that of yoke. For sinusoidal power supply and rated load motor, the iron loss density near the tooth gap is greater than 120 W/kg, and the iron loss density at the yoke of the rotor is less than 0.05 W/kg (as shown in Fig. 9).

Figure 10 depicts the change of calculated iron loss with switching frequency and its comparison with measured values. As can be seen from Fig. 10, with the increase of switching frequency, iron loss decreases from 115 W at 1 K to 103 W at 5 K, decreasing by 10.43%. In addition, it can be seen from Fig. 10 that the PVCIL model also has high accuracy under the condition of PWM power supply. The hysteresis loss and eddy current loss of iron loss at different switching frequencies are obtained through PVCIL model. It can be seen from Fig. 10 that the hysteresis loss decreases slightly with the increase of the switching frequency of the frequency converter, from 52 W at 1 K to 50 W at 5 K, reduced by 3.8%. The eddy current loss decreases greatly with the increase of the switching frequency, from 60 W at 1 K to 52 W at 5 K, reduced by 13.3%.

6. CONCLUSIONS

In this study, the topic of motor iron loss is discussed in detail. The purpose of this study is to provide references and ideas for high-efficiency motor design and high-efficiency motor system control. In this paper, the influences of various factors on iron loss are discussed in detail from the aspects of power supply, material composition, motor structure, multiphysics, and manufacturing processes of the motor core. By summarizing the factors affecting iron loss, it can provide energy-saving ways for designers in the selection of ferromagnetic materials, frequency converter, machining processing, motor structure, etc. The advantages and disadvantages of different iron loss models are discussed, and different types of iron loss models are summarized, which can help the motor designer to choose the iron loss calculation model reasonably, so as to optimize the motor structure in the motor design stage, and help the system control designer to deduce the optimal efficiency control algorithm. The discussion of the existing methods of measuring iron loss is helpful to standardize the measurement of the efficiency of converter-fed motors.

ACKNOWLEDGEMENT

This work was supported in part by the National Natural Science Foundation of China (52107083), and the Guangxi Science and Technology Base and Talent Special Project of China

(GuikeAD21220143), and the Innovation Project of Guangxi Graduate Education (YCBZ2024005).

REFERENCES

[1] Ren, M., P. Lu, X. Liu, M. S. Hossain, Y. Fang, T. Hanaoka, B. O'Gallachoir, J. Glynn, and H. Dai, "Decarbonizing China's iron and steel industry from the supply and demand sides for carbon neutrality," *Applied Energy*, Vol. 298, 117209, 2021.

[2] De Almeida, A., J. Fong, C. U. Brunner, R. Werle, and M. V. Werkhoven, "New technology trends and policy needs in energy efficient motor systems — A major opportunity for energy and carbon savings," *Renewable and Sustainable Energy Reviews*, Vol. 115, 109384, 2019.

[3] Zhu, X., D. Fan, Z. Xiang, L. Quan, W. Hua, and M. Cheng, "Systematic multi-level optimization design and dynamic control of less-rare-earth hybrid permanent magnet motor for all-climatic electric vehicles," *Applied Energy*, Vol. 253, 113549, 2019.

[4] Trianni, A., E. Cagno, and D. Accordini, "Energy efficiency measures in electric motors systems: A novel classification highlighting specific implications in their adoption," *Applied Energy*, Vol. 252, 113481, 2019.

[5] Saidur, R., "A review on electrical motors energy use and energy savings," *Renewable and Sustainable Energy Reviews*, Vol. 14, No. 3, 877–898, 2010.

[6] Yan, S., M. Gao, J. Zhang, M. Xu, Y. Zhang, and W. Wang, "Effect of stator on core loss of the embedded combined magnetic pole drive motor for new energy vehicles," *Progress In Electromagnetics Research C*, Vol. 127, 207–225, 2022.

[7] Li, K., A. Xu, B. Leng, Y. Yang, and J. Sun, "Iron loss calculation in switched reluctance motor based on flux integral path method," *Progress In Electromagnetics Research M*, Vol. 112, 151–161, 2022.

[8] Wang, X., M. Reitz, and E. E. Yaz, "Field oriented sliding mode control of surface-mounted permanent magnet AC motors: Theory and applications to electrified vehicles," *IEEE Transactions on Vehicular Technology*, Vol. 67, No. 11, 10 343–10 356, 2018.

[9] Alzayed, M. and H. Chaoui, "Efficient simplified current sensorless dynamic direct voltage MTPA of interior PMSM for electric vehicles operation," *IEEE Transactions on Vehicular Technology*, Vol. 71, No. 12, 12 701–12 710, 2022.

[10] Cho, Y., Y. Bak, and K.-B. Lee, "Torque-ripple reduction and fast torque response strategy for predictive torque control of induction motors," *IEEE Transactions on Power Electronics*, Vol. 33, No. 3, 2458–2470, 2018.

[11] Krings, A. and J. Soulard, "Overview and comparison of iron loss models for electrical machines," *Journal of Electrical Engineering*, Vol. 10, No. 3, 162–169, 2010.

[12] Akiror, J. C., T. Rahman, and P. Pillay, "Progress on formulas for core loss calculations," in *2012 XXth International Conference on Electrical Machines*, 1803–1809, Marseille, France, 2012.

[13] Li, Z., W. Han, Z. Xin, Q. Liu, J. Chen, and P. C. Loh, "A review of magnetic core materials, core loss modeling and measurements in high-power high-frequency transformers," *CPSS Transactions on Power Electronics and Applications*, Vol. 7, No. 4, 359–373, 2022.

[14] Rodriguez-Sotelo, D., M. A. Rodriguez-Licea, I. Araujo-Vargas, J. Prado-Olivarez, A.-I. Barranco-Gutiérrez, and F. J. Perez-Pinal, "Power losses models for magnetic cores: A review," *Micromachines*, Vol. 13, No. 3, 418, 2022.

[15] Guo, Y., J. G. Zhu, J. Zhong, H. Lu, and J. X. Jin, "Measurement and modeling of rotational core losses of soft magnetic materials used in electrical machines: A review," *IEEE Transactions on Magnetics*, Vol. 44, No. 2, 279–291, 2008.

[16] Liu, G., M. Liu, Y. Zhang, H. Wang, and C. Gerada, "High-speed permanent magnet synchronous motor iron loss calculation method considering multiphysics factors," *IEEE Transactions on Industrial Electronics*, Vol. 67, No. 7, 5360–5368, 2020.

[17] Zhang, H., M. Dou, and J. Deng, "Loss-minimization strategy of nonsinusoidal back EMF PMSM in multiple synchronous reference frames," *IEEE Transactions on Power Electronics*, Vol. 35, No. 8, 8335–8346, 2020.

[18] Hang, J., H. Wu, S. Ding, Y. Huang, and W. Hua, "Improved loss minimization control for IPMSM using equivalent conversion method," *IEEE Transactions on Power Electronics*, Vol. 36, No. 2, 1931–1940, 2021.

[19] Sundaria, R., D. G. Nair, A. Lehikoinen, A. Arkkio, and A. Belahcen, "Effect of laser cutting on core losses in electrical machines — Measurements and modeling," *IEEE Transactions on Industrial Electronics*, Vol. 67, No. 9, 7354–7363, 2020.

[20] Cavagnino, A. and A. Boglietti, "Iron loss prediction with PWM supply: An overview of proposed methods from an engineering application point of view," in *2007 IEEE Industry Applications Annual Meeting*, 81–88, New Orleans, LA, USA, 2007.

[21] Boglietti, A., A. Cavagnino, T. L. Mthombeni, and P. Pillay, "Comparison of lamination iron losses supplied by PWM voltages: US and European experiences," in *IEEE International Conference on Electric Machines and Drives, 2005*, 1431–1436, San Antonio, TX, USA, 2005.

[22] Vidal, N., K. Gandarias, G. Almandoz, and J. Poza, "Determination of the magnetic losses in laminated cores under pulse width modulation voltage supply," *The Physics of Metals and Metallography*, Vol. 116, 774–780, 2015.

[23] Xue, S., J. Feng, S. Guo, Z. Chen, J. Peng, W. Q. Chu, P. L. Xu, and Z. Q. Zhu, "Iron loss model for electrical machine fed by low switching frequency inverter," *IEEE Transactions on Magnetics*, Vol. 53, No. 11, 1–4, 2017.

[24] Arish, N., M. Ardestani, and A. Hekmati, "Optimum structure of rotor slot for a 20 kW HTS induction motor," *Physica C: Superconductivity and Its Applications*, Vol. 582, 1353829, 2021.

[25] Marčič, T., B. Štumberger, G. Štumberger, M. Hadžiselimović, and I. Zagradišnik, "The impact of different stator and rotor slot number combinations on iron losses of a three-phase induction motor at no-load," *Journal of Magnetism and Magnetic Materials*, Vol. 320, No. 20, e891–e895, 2008.

[26] Chakkarapani, K., T. Thangavelu, K. Dharmalingam, and P. Thandavarayan, "Multiobjective design optimization and analysis of magnetic flux distribution for slotless permanent magnet brushless DC motor using evolutionary algorithms," *Journal of Magnetism and Magnetic Materials*, Vol. 476, 524–537, 2019.

[27] Bache-Wiig, J., "Application of fractional pitch windings to alternating-current generators," *Proceedings of the American Institute of Electrical Engineers*, Vol. 27, No. 5, 657–665, 1908.

[28] Fan, X., B. Zhang, R. Qu, D. Li, J. Li, and Y. Huo, "Comparative thermal analysis of IPMSMs with integral-slot distributed-winding (ISDW) and fractional-slot concentrated-winding (FSCW) for electric vehicle application," *IEEE Transactions on Industry Applications*, Vol. 55, No. 4, 3577–3588, 2019.

[29] Zhao, W., J. Zheng, J. Ji, S. Zhu, and M. Kang, "Star and delta hybrid connection of a FSCW PM machine for low space harmonics," *IEEE Transactions on Industrial Electronics*, Vol. 65, No. 12, 9266–9279, 2018.

[30] Islam, M. S., M. A. Kabir, R. Mikail, and I. Husain, "Space-shifted wye-delta winding to minimize space harmonics of fractional-slot winding," *IEEE Transactions on Industry Applications*, Vol. 56, No. 3, 2520–2530, 2020.

[31] Dajaku, G., W. Xie, and D. Gerling, "Reduction of low space harmonics for the fractional slot concentrated windings using a novel stator design," *IEEE Transactions on Magnetics*, Vol. 50, No. 5, 1–12, 2014.

[32] Yamazaki, K. and H. Ishigami, "Rotor-shape optimization of interior-permanent-magnet motors to reduce harmonic iron losses," *IEEE Transactions on Industrial Electronics*, Vol. 57, No. 1, 61–69, 2010.

[33] Yang, Z., S. Wang, Y. Sun, and H. Cao, "Vibration reduction by magnetic slot wedge for rotating armature permanent magnet motors," *IEEE Transactions on Industry Applications*, Vol. 56, No. 5, 4882–4888, 2020.

[34] Zhao, P., J. Pan, B. Zhao, and J. Wu, "Molecular dynamics study of crystal orientation effect on surface generation mechanism of single-crystal silicon during the nano-grinding process," *Journal of Manufacturing Processes*, Vol. 74, 190–200, 2022.

[35] Da C. Paolinelli, S., M. A. Da Cunha, S. S. F. De Dafe, and A. B. Cota, "Study of the simultaneous effects of the hot band grain size and cold rolling reduction on the structure and magnetic properties of nonoriented 3Si steel," *IEEE Transactions on Magnetics*, Vol. 48, No. 4, 1401–1404, 2012.

[36] Oda, Y., H. Toda, N. Shiga, S. Kasai, and T. Hiratani, "Effect of Si content on iron loss of electrical steel sheet under compressive stress," *IEEE Transactions on Magnetics*, Vol. 50, No. 4, 1–4, 2014.

[37] Krings, A., M. Cossale, A. Tenconi, J. Soulard, A. Cavagnino, and A. Boglietti, "Magnetic materials used in electrical machines: A comparison and selection guide for early machine design," *IEEE Industry Applications Magazine*, Vol. 23, No. 6, 21–28, 2017.

[38] Krings, A., A. Boglietti, A. Cavagnino, and S. Sprague, "Soft magnetic material status and trends in electric machines," *IEEE Transactions on Industrial Electronics*, Vol. 64, No. 3, 2405–2414, 2017.

[39] Boglietti, A., A. M. El-Refaie, O. Drubel, A. M. Omekanda, N. Bianchi, E. B. Agamloh, M. Popescu, A. D. Gerlando, and J. B. Bartolo, "Electrical machine topologies: Hottest topics in the electrical machine research community," *IEEE Industrial Electronics Magazine*, Vol. 8, No. 2, 18–30, 2014.

[40] Paltanea, G., V. Manescu, A. Antoniac, I. V. Nemoianu, and H. Gavrila, "Mechanical and magnetic properties variation in non-oriented electrical steels with different cutting technology: A review," *Materials*, Vol. 17, No. 6, 1345, 2024.

[41] Sundaria, R., A. Lehikoinen, A. Arkkio, and A. Belahcen, "Effects of manufacturing processes on core losses of electrical machines," *IEEE Transactions on Energy Conversion*, Vol. 36, No. 1, 197–206, 2021.

[42] Harstick, H. M. S., M. Ritter, and W. Riehemann, "Influence of punching and tool wear on the magnetic properties of nonoriented electrical steel," *IEEE Transactions on Magnetics*, Vol. 50, No. 4, 1–4, 2014.

[43] Bali, M. and A. Muetze, "Influences of CO2 Laser, FKL laser, and mechanical cutting on the magnetic properties of electrical steel sheets," *IEEE Transactions on Industry Applications*, Vol. 51, No. 6, 4446–4454, 2015.

[44] Singh, S., A. Credo, I. Petrov, J. Pyrhönen, and P. Lindh, "Impact of laser cutting on iron loss in high speed machines," *Progress In Electromagnetics Research C*, Vol. 141, 67–78, 2024.

[45] Saleem, A., N. Alatawneh, T. Rahman, D. A. Lowther, and R. R. Chromik, "Effects of laser cutting on microstructure and magnetic properties of non-orientation electrical steel laminations," *IEEE Transactions on Magnetics*, Vol. 56, No. 12, 1–9, 2020.

[46] Dems, M., Z. Gmyrek, and K. Komeza, "The influence of cutting technology on magnetic properties of non-oriented electrical steel — Review state of the art," *Energies*, Vol. 16, No. 11, 4299, 2023.

[47] Bali, M. and A. Muetze, "The degradation depth of non-grain oriented electrical steel sheets of electric machines due to mechanical and laser cutting: A state-of-the-art review," *IEEE Transactions on Industry Applications*, Vol. 55, No. 1, 366–375, Jan.–Feb. 2019.

[48] Xue, S., J. Feng, S. Guo, J. Peng, W. Q. Chu, and Z. Q. Zhu, "A new iron loss model for temperature dependencies of hysteresis and eddy current losses in electrical machines," *IEEE Transactions on Magnetics*, Vol. 54, No. 1, 1–10, 2018.

[49] Liu, S., T. Li, J. Luo, Y. Yang, C. Liu, and Y. Wang, "Core loss analysis of soft magnetic composites based on 3D model considering temperature influence," *IEEE Access*, Vol. 9, 153 420–153 428, 2021.

[50] Chen, J., D. Wang, Y. Jiang, X. Teng, S. Cheng, and J. Hu, "Examination of temperature-dependent iron loss models using a stator core," *IEEE Transactions on Magnetics*, Vol. 54, No. 11, 1–7, 2018.

[51] Liu, L., X. Ba, Y. Guo, G. Lei, X. Sun, and J. Zhu, "Improved iron loss prediction models for interior PMSMs considering coupling effects of multiphysics factors," *IEEE Transactions on Transportation Electrification*, Vol. 9, No. 1, 416–427, 2023.

[52] Yamazaki, K. and H. Takeuchi, "Impact of mechanical stress on characteristics of interior permanent magnet synchronous motors," *IEEE Transactions on Industry Applications*, Vol. 53, No. 2, 963–970, 2017.

[53] Yamazaki, K. and Y. Kato, "Iron loss analysis of interior permanent magnet synchronous motors by considering mechanical stress and deformation of stators and rotors," *IEEE Transactions on Magnetics*, Vol. 50, No. 2, 909–912, 2014.

[54] Zhang, Z., A. Nysveen, B. J. Fagermyr, A. Chen, H. Ehya, and R. Nilssen, "Material characterization and stator core loss computation of synchronous generators with stacking force accounted," *IEEE Transactions on Industry Applications*, Vol. 60, No. 1, 239–248, Jan.-Feb. 2024.

[55] Steinmetz, C. P., "On the law of hysteresis," *Proceedings of the IEEE*, Vol. 72, No. 2, 197–221, 1984.

[56] Reinert, J., A. Brockmeyer, and R. W. A. A. D. Doncker, "Calculation of losses in ferro-and ferrimagnetic materials based on the modified steinmetz equation," *IEEE Transactions on Industry Applications*, Vol. 37, No. 4, 1055–1061, Jul. 2001.

[57] Li, J., T. Abdallah, and C. R. Sullivan, "Improved calculation of core loss with nonsinusoidal waveforms," in *Conference Record of the 2001 IEEE Industry Applications Conference. 36th IAS Annual Meeting (Cat. No.01CH37248)*, Vol. 4, 2203–2210, Chicago, IL, USA, 2001.

[58] Venkatachalam, K., C. R. Sullivan, T. Abdallah, and H. Tacca, "Accurate prediction of ferrite core loss with nonsinusoidal waveforms using only steinmetz parameters," in *2002 IEEE Workshop on Computers in Power Electronics, 2002. Proceed-*

ings., 36–41, Mayaguez, PR, USA, 2002.

[59] Bossche, Van den A., V. C. Valchev, and G. B. Georgiev, "Measurement and loss model of ferrites with non-sinusoidal waveforms," in *2004 IEEE 35th Annual Power Electronics Specialists Conference (IEEE Cat. No.04CH37551)*, Vol. 6, 4814–4818, Aachen, Germany, 2004.

[60] Alsawalhi, J. Y. and S. D. Sudhoff, "Saturable thermally-representative steinmetz-based loss models," *IEEE Transactions on Magnetics*, Vol. 49, No. 11, 5438–5445, 2013.

[61] Jordan, H., "Die ferromagnetischen Konstanten für schwache Wechselfelder," *Elektr. Nach. Techn*, Vol. 1, No. 8, 1924.

[62] Bertotti, G., "General properties of power losses in soft ferromagnetic materials," *IEEE Transactions on Magnetics*, Vol. 24, No. 1, 621–630, 1988.

[63] Moses, A. J., "Importance of rotational losses in rotating machines and transformers," *Journal of Materials Engineering and Performance*, Vol. 1, No. 2, 235–244, 1992.

[64] Kochmann, T., "Relationship between rotational and alternating losses in electrical steel sheets," *Journal of Magnetism and Magnetic Materials*, Vol. 160, 145–146, 1996.

[65] Zhang, D., H. Zhao, and T. Wu, "The rotor copper and iron loss analysis of inverter-fed induction motor considering rotor slip frequency," in *2017 IEEE Energy Conversion Congress and Exposition (ECCE)*, 2412–2419, Cincinnati, OH, USA, 2017.

[66] Boglietti, A., A. Cavagnino, M. Lazzari, and M. Pastorelli, "Predicting iron losses in soft magnetic materials with arbitrary voltage supply: An engineering approach," *IEEE Transactions on Magnetics*, Vol. 39, No. 2, 981–989, 2003.

[67] Steentjes, S., G. v. Pfingsten, M. Hombitzer, and K. Hameyer, "Iron-loss model with consideration of minor loops applied to FE-simulations of electrical machines," *IEEE Transactions on Magnetics*, Vol. 49, No. 7, 3945–3948, 2013.

[68] Eggers, D., S. Steentjes, and K. Hameyer, "Advanced iron-loss estimation for nonlinear material behavior," *IEEE Transactions on Magnetics*, Vol. 48, No. 11, 3021–3024, 2012.

[69] Ionel, D. M., M. Popescu, S. J. Dellinger, T. J. E. Miller, R. J. Heideman, and M. I. McGilp, "On the variation with flux and frequency of the core loss coefficients in electrical machines," *IEEE Transactions on Industry Applications*, Vol. 42, No. 3, 658–667, 2006.

[70] Popescu, M. and D. M. Ionel, "A best-fit model of power losses in cold rolled-motor lamination steel operating in a wide range of frequency and magnetization," *IEEE Transactions on Magnetics*, Vol. 43, No. 4, 1753–1756, 2007.

[71] Upadhyay, T., J. Ding, and N. H. Rhee, "A piecewise quadratic maximum entropy method for the statistical study of chaos," *Journal of Mathematical Analysis and Applications*, Vol. 421, No. 2, 1487–1501, Jan. 2015.

[72] Zhao, H., Y. Wang, D. Zhang, Y. Zhan, G. Xu, and Y. Luo, "Piecewise variable parameter model for precise analysis of iron losses in induction motors," *IET Electric Power Applications*, Vol. 11, No. 3, 361–368, 2017.

[73] Zhao, H., D. Zhang, Y. Wang, Y. Zhan, and G. Xu, "Piecewise variable parameter loss model of laminated steel and its application in fine analysis of iron loss of inverter-fed induction motors," *IEEE Transactions on Industry Applications*, Vol. 54, No. 1, 832–840, 2018.

[74] Du, G., W. Xu, J. Zhu, and N. Huang, "Power loss and thermal analysis for high-power high-speed permanent magnet machines," *IEEE Transactions on Industrial Electronics*, Vol. 67, No. 4, 2722–2733, 2020.

[75] Leandro, M., N. Elloumi, A. Tessarolo, and J. K. Nøland, "Analytical iron loss evaluation in the stator yoke of slotless surface-mounted PM machines," *IEEE Transactions on Industry Applications*, Vol. 58, No. 4, 4602–4613, 2022.

[76] Bi, L., U. Schäfer, and Y. Hu, "A new high-frequency iron loss model including additional iron losses due to punching and burrs' connection," *IEEE Transactions on Magnetics*, Vol. 56, No. 10, 1–9, 2020.

[77] Zhao, H., H. H. Eldeeb, Y. Zhang, D. Zhang, Y. Zhan, G. Xu, and O. A. Mohammed, "An improved core loss model of ferromagnetic materials considering high-frequency and nonsinusoidal supply," *IEEE Transactions on Industry Applications*, Vol. 57, No. 4, 4336–4346, 2021.

[78] Zhu, Z.-Q., S. Xue, W. Chu, J. Feng, S. Guo, Z. Chen, and J. Peng, "Evaluation of iron loss models in electrical machines," *IEEE Transactions on Industry Applications*, Vol. 55, No. 2, 1461–1472, 2019.

[79] Zhu, S. and B. Shi, "Modeling of PWM-induced iron losses with frequency-domain methods and low-frequency parameters," *IEEE Transactions on Industrial Electronics*, Vol. 69, No. 3, 2402–2413, 2022.

[80] Moses, A., "Effects of magnetic properties and geometry on flux harmonics and losses in 3-phase, 5-limb, split-limb, transformer cores," *IEEE Transactions on Magnetics*, Vol. 23, No. 5, 3780–3782, 1987.

[81] Karakos, D. and A. Papamarcou, "A relationship between quantization and watermarking rates in the presence of additive gaussian attacks," *IEEE Transactions on Information Theory*, Vol. 49, No. 8, 1970–1982, 2003.

[82] Birčáková, Z., P. Kollár, J. Füzer, R. Bureš, and M. Fáberová, "Magnetic properties of selected Fe-based soft magnetic composites interpreted in terms of Jiles-Atherton model parameters," *Journal of Magnetism and Magnetic Materials*, Vol. 502, 166514, 2020.

[83] Antonio, S. Q., A. M. Ghanim, A. Faba, and A. Laudani, "Numerical simulations of vector hysteresis processes via the Preisach model and the Energy Based Model: An application to Fe-Si laminated alloys," *Journal of Magnetism and Magnetic Materials*, Vol. 539, 168372, 2021.

[84] Ruderman, M. and T. Bertram, "Identification of soft magnetic BH characteristics using discrete dynamic Preisach model and single measured hysteresis loop," *IEEE Transactions on Magnetics*, Vol. 48, No. 4, 1281–1284, 2012.

[85] Messal, O., A. T. Vo, M. Fassenet, P. Mas, S. Buffat, and A. Kedous-Lebouc, "Advanced approach for static part of loss-surface iron loss model," *Journal of Magnetism and Magnetic Materials*, Vol. 502, 166401, 2020.

[86] Dlala, E., A. Belahcen, and A. Arkkio, "Efficient magnetodynamic lamination model for two-dimensional field simulation of rotating electrical machines," *Journal of Magnetism and Magnetic Materials*, Vol. 320, No. 20, e1006–e1010, 2008.

[87] Mayergoyz, I. D., *Mathematical Models of Hysteresis and Their Applications*, Academic Press, 2003.

[88] Scorretti, R. and F. Sixdenier, "An analytical formula to identify the parameters of the energy-based hysteresis model," *Journal of Magnetism and Magnetic Materials*, Vol. 548, 168748, 2022.

[89] Philips, D. A., L. R. Dupre, and J. A. Melkebeek, "Comparison of Jiles and Preisach hysteresis models in magnetodynamics," *IEEE Transactions on Magnetics*, Vol. 31, No. 6, 3551–3553, 1995.

[90] Benabou, A., S. Clénet, and F. Piriou, "Comparison of Preisach and Jiles-Atherton models to take into account hysteresis phenomenon for finite element analysis," *Journal of Magnetism and Magnetic Materials*, Vol. 261, No. 1–2, 139–160, 2003.

[91] Li, Y., J. Zhu, Y. Li, and L. Zhu, "A hybrid Jiles-Atherton and Preisach model of dynamic magnetic hysteresis based on back-propagation neural networks," *Journal of Magnetism and Magnetic Materials*, Vol. 544, No. 15, 168655, 2022.

[92] Riccardo, S., F. Riganti-Fulginei, A. Laudani, and S. Quandam, "Algorithms to reduce the computational cost of vector Preisach model in view of finite element analysis," *Journal of Magnetism and Magnetic Materials*, Vol. 546, 168876, 2022.

[93] Hussain, S. and D. A. Lowther, "An efficient implementation of the classical Preisach model," *IEEE Transactions on Magnetics*, Vol. 54, No. 3, 1–4, 2018.

[94] Tousignant, M., F. Sirois, G. Meunier, and C. Guérin, "Incorporation of a vector Preisach–Mayergoyz hysteresis model in 3-D finite element analysis," *IEEE Transactions on Magnetics*, Vol. 55, No. 6, 1–4, 2019.

[95] Won, H., H. Ju, S. Park, and G. Park, "A study on the deperming of a ferromagnetic material by using Preisach model with M-B variables," *IEEE Transactions on Magnetics*, Vol. 49, No. 5, 2045–2048, 2013.

[96] Kuczmann, M. and G. Kovács, "Improvement and application of the viscous-type frequency-dependent Preisach model," *IEEE Transactions on Magnetics*, Vol. 50, No. 2, 385–388, 2014.

[97] Zhu, L., W. Wu, X. Xu, Y. Guo, W. Li, K. Lu, and C.-S. Koh, "An improved anisotropic vector Preisach hysteresis model taking account of rotating magnetic fields," *IEEE Transactions on Magnetics*, Vol. 55, No. 6, 1–4, 2019.

[98] Fallah, E. and J. S. Moghani, "A new identification and implementation procedure for the isotropic vector Preisach model," *IEEE Transactions on Magnetics*, Vol. 44, No. 1, 37–42, 2008.

[99] Mayergoyz, I. D. and G. Friedman, "Isotropic vector Preisach model of hysteresis," *Journal of Applied Physics*, Vol. 61, No. 8, 4022–4024, 1987.

[100] Zhao, X., H. Xu, Y. Li, L. Zhou, X. Liu, H. Zhao, Y. Liu, and D. Yuan, "Improved Preisach model for the vector hysteresis property of soft magnetic composite materials based on the hybrid technique of SA-NMS," *IEEE Transactions on Industry Applications*, Vol. 57, No. 5, 5517–5526, 2021.

[101] Mathekga, M. E., R. A. McMahon, and A. M. Knight, "Application of the fixed point method for solution in time stepping finite element analysis using the inverse vector Jiles-Atherton model," *IEEE Transactions on Magnetics*, Vol. 47, No. 10, 3048–3051, 2011.

[102] Perkkiö, L., B. Upadhaya, A. Hannukainen, and P. Rasilo, "Stable adaptive method to solve FEM coupled with Jiles-Atherton hysteresis model," *IEEE Transactions on Magnetics*, Vol. 54, No. 2, 1–8, 2018.

[103] Hoffmann, K., J. P. A. Bastos, J. V. Leite, N. Sadowski, and F. Barbosa, "A vector Jiles-Atherton model for improving the FEM convergence," *IEEE Transactions on Magnetics*, Vol. 53, No. 6, 1–4, 2017.

[104] Hamimid, M., M. Feliachi, and S. M. Mimoune, "Modified Jiles-Atherton model and parameters identification using false position method," *Physica B: Condensed Matter*, Vol. 405, No. 8, 1947–1950, Apr. 2010.

[105] Padilha, J. B., P. Kuo-Peng, N. Sadowski, J. V. Leite, and N. J. Batistela, "Restriction in the determination of the Jiles-Atherton hysteresis model parameters," *Journal of Magnetism and Magnetic Materials*, Vol. 442, 8–14, 2017.

[106] Upadhaya, B., P. Rasilo, L. Perkkiö, P. Handgruber, A. Benabou, A. Belahcen, and A. Arkkio, "Alternating and rotational loss prediction accuracy of vector Jiles-Atherton model," *Journal of Magnetism and Magnetic Materials*, Vol. 527, 167690, 2021.

[107] Li, W., I. H. Kim, S. M. Jang, and C. S. Koh, "Hysteresis modeling for electrical steel sheets using improved vector Jiles-Atherton hysteresis model," *IEEE Transactions on Magnetics*, Vol. 47, No. 10, 3821–3824, 2011.

[108] Liu, Y., X. Gao, and Y. Li, "Giant magnetostrictive actuator nonlinear dynamic Jiles-Atherton model," *Sensors and Actuators A: Physical*, Vol. 250, 7–14, 2016.

[109] Sarker, P. C., Y. Guo, H. Lu, and J. G. Zhu, "Improvement on parameter identification of modified Jiles-Atherton model for iron loss calculation," *Journal of Magnetism and Magnetic Materials*, Vol. 542, 168602, 2022.

[110] Hussain, S. and D. A. Lowther, "Prediction of iron losses using Jiles-Atherton model with interpolated parameters under the conditions of frequency and compressible stress," *IEEE Transactions on Magnetics*, Vol. 52, No. 3, 730040, 2016.

[111] Li, Y., L. Zhu, and J. Zhu, "Core loss calculation based on finite-element method with Jiles-Atherton dynamic hysteresis model," *IEEE Transactions on Magnetics*, Vol. 54, No. 3, 1–5, 2018.

[112] Zhang, D., T. Liu, H. Zhao, and T. Wu, "An analytical iron loss calculation model of inverter-fed induction motors considering supply and slot harmonics," *IEEE Transactions on Industrial Electronics*, Vol. 66, No. 12, 9194–9204, 2019.

[113] Zhang, D., J. Yi, X. Li, T. Liu, H. Zhao, Y. Zhang, and T. Wu, "Core loss equivalent resistance modeling of small-and medium-sized converter-fed induction motors considering supply and spatial harmonics," *IEEE Transactions on Industrial Electronics*, Vol. 70, No. 9, 8768–8776, 2022.

[114] Minowa, N., Y. Takahashi, and K. Fujiwara, "Iron loss analysis of interior permanent magnet synchronous motors using dynamic hysteresis model represented by Cauer circuit," *IEEE Transactions on Magnetics*, Vol. 55, No. 6, 1–4, 2019.

[115] Balamurali, A., A. Kundu, Z. Li, and N. C. Kar, "Improved harmonic iron loss and stator current vector determination for maximum efficiency control of PMSM in EV applications," *IEEE Transactions on Industry Applications*, Vol. 57, No. 1, 363–373, 2021.

[116] Liu, Y. and A. M. Bazzi, "A general analytical three-phase induction machine core loss model in the arbitrary reference frame," *IEEE Transactions on Industry Applications*, Vol. 53, No. 5, 4210–4220, 2017.

[117] Kuttler, S., K. E. K. Benkara, G. Friedrich, A. Abdelli, and F. Vangraefschepe, "Fast iron losses model of stator taking into account the flux weakening mode for the optimal sizing of high speed permanent internal magnet synchronous machine," *Mathematics and Computers in Simulation*, Vol. 131, 328–343, 2017.

[118] Djelloul-Khedda, Z., K. Boughrara, F. Dubas, A. Kechroud, and A. Tikellaline, "Analytical prediction of iron-core losses in flux-modulated permanent-magnet synchronous machines," *IEEE Transactions on Magnetics*, Vol. 55, No. 1, 1–12, 2018.

[119] Liu, R. and L. Li, "Analytical prediction model of energy losses in soft magnetic materials over broadband frequency range," *IEEE Transactions on Power Electronics*, Vol. 36, No. 2, 2009–2017, 2021.

[120] Desvaux, M., S. Sire, S. Hlioui, H. B. Ahmed, and B. Multon, "Development of a hybrid analytical model for a fast computation of magnetic losses and optimization of coaxial magnetic gears," *IEEE Transactions on Energy Conversion*, Vol. 34, No. 1, 25–35, 2019.

[121] Liang, P., Y. Tang, F. Chai, K. Shen, and W. Liu, "Calculation of the iron losses in a spoke-type permanent magnet

synchronous in-wheel motor for electric vehicles by utilizing the bertotti model," *IEEE Transactions on Magnetics*, Vol. 55, No. 7, 1–7, 2019.

[122] Cao, W., "Comparison of ieee 112 and new iec standard 60034-2-1," *IEEE Transactions on Energy Conversion*, Vol. 24, No. 3, 802–808, 2009.

[123] Karkkainen, H., L. Aarniovuori, M. Niemela, and J. Pyrhonen, "Converter-fed induction motor efficiency: Practical applicability of IEC methods," *IEEE Industrial Electronics Magazine*, Vol. 11, No. 2, 45–57, 2017.

[124] Antonello, R., F. Tinazzi, and M. Zigliotto, "Energy efficiency measurements in IM: The non-trivial application of the norm IEC 60034-2-3: 2013," in *2015 IEEE Workshop on Electrical Machines Design, Control and Diagnosis (WEMDCD)*, 248–253, Turin, Italy, 2015.

[125] Agamloh, E. B., A. Cavagnino, and S. Vaschetto, "Standard efficiency determination of induction motors with a PWM inverter source," *IEEE Transactions on Industry Applications*, Vol. 55, No. 1, 398–406, 2019.

[126] Chirindo, M., M. A. Khan, and P. S. Barendse, "Considerations for nonintrusive efficiency estimation of inverter-fed induction motors," *IEEE Transactions on Industrial Electronics*, Vol. 63, No. 2, 741–749, 2016.

[127] Mushenya, J., M. A. Khan, and P. S. Barendse, "Development of a test rig to automate efficiency testing of converter-fed induction motors," *IEEE Transactions on Industry Applications*, Vol. 55, No. 6, 5916–5924, 2019.

[128] Dems, M., K. Komeza, and J.-P. Lecointe, "Variation of additional losses at no-load and full-load for a wide range of rated power induction motors," *Electric Power Systems Research*, Vol. 143, 692–702, 2017.

[129] Leitner, S., G. Krenn, H. Gruebler, and A. Muetze, "Rheometer-based cogging and hysteresis torque and iron loss determination of sub-fractional horsepower motors," *IEEE Transactions on Industry Applications*, Vol. 56, No. 4, 3679–3690, 2020.

[130] Boubaker, N., D. Matt, P. Enrici, F. Nierlich, and G. Durand, "Measurements of iron loss in PMSM stator cores based on CoFe and SiFe lamination sheets and stemmed from different manufacturing processes," *IEEE Transactions on Magnetics*, Vol. 55, No. 1, 1–9, 2019.